Biosensors and Bioelectronics 46 (2013) 61–67

Contents lists available at SciVerse ScienceDirect

Biosensors and Bioelectronics

journal homepage: www.elsevier.com/locate/bios

Acetylcholinesterase biosensor for carbamate drugs based on tetrathiafulvalene–tetracyanoquinodimethane/ionic liquid conductive gels

Lucian-Gabriel Zamfir [a,b], Lucian Rotariu [a,b], Camelia Bala [a,b,*]

[a] Department of Analytical Chemistry, University of Bucharest, 4-12 Regina Elisabeta Blvd., 030018 Bucharest, Romania
[b] LaborQ, University of Bucharest, 4-12 Regina Elisabeta Blvd., 030018 Bucharest, Romania

ARTICLE INFO

Article history:
Received 24 November 2012
Received in revised form
8 February 2013
Accepted 11 February 2013
Available online 27 February 2013

Keywords:
Drug
Eserine
Neostigmine
TCNQ–TTF
Ionic liquid
Biosensor

ABSTRACT

A highly sensitive acetylcholinesterase biosensor was developed for detection of carbamate drugs based on TTF–TCNQ–ionic liquid gel thiocholine sensor. The TTF–TCNQ–ionic/ionic liquid gel was characterized by FT-IR and scanning electron microscopy. The electrocatalytic behavior of TTF–TCNQ–ionic liquid gels toward oxidation of thiocholine was thoroughly investigated. 1-Ethyl-3-methylimidazolium tetracyanoborate gel based sensor allowed amperometric detection of thiocholine at +400 mV vs. Ag/AgCl with a high sensitivity of 55.9 ± 1.2 μA mM^{-1} cm^{-2} and a low detection limit equal to 7.6 μM. The catalytic rate constant and diffusion constant of thiocholine were estimated from chronoamperometric data. The proposed biosensor based on AChE immobilized in sol–gel matrix was used for the detection of two carbamate therapeutic drugs. Very low detection limits of 26 pM eserine and 0.3 nM neostigmine were achieved. The analysis of spiked tap water proved the biosensor capability to be used as a screening method for detection of carbamate drugs in wastewaters.

1. Introduction

Neostigmine and eserine (physostigmine) are carbamate drugs acting as acetylcholinesterase (AChE) inhibitors. They bind at both the anionic and esteric sites of AChE, forming a drug–enzyme complex, as the enzyme substrate and the organophosphates do (Wilson et al., 1961). Many studies suggest that the mechanism is not completely reversible (Darvesh et al., 2003; Ghous and Townshend, 1998).

The presence in the waste water of drug residues which act as AChE inhibitor is a major problem due to their potential toxicity toward humans and animals and therefore a sensitive and fast detection is of great importance (LeDoux, 2011). The analytical methods reported in the literature for the detection of eserine include the capillary electrophoresis (Havel et al., 2002), HPLC (Rubnov et al., 1999), and flow injection with spectrophotometric detection (Ghous and Townshend, 1998), HPLC (Varin et al., 1999) or surface plasmon resonance (Milkani et al., 2011) for detection of neostigmine. All this techniques need an elaborated sampling protocol, expensive equipment and could not be used on field measurement. Biosensors offer the advantage of low detection limits with short analysis time, without any sampling preparation, and they could be integrated in portable systems. The most reported electrochemical biosensors based on AChE inhibition have been used mainly for toxic compounds detection (Amine et al., 2006; Andreescu and Marty, 2006). Only few electrochemical biosensors are reported in the literature for carbamate drugs detection. A bienzymatic amperometric biosensor, having avidin-modified AChE and choline oxidase (ChO) immobilized on a metal supported biotinylated membrane achieved a detection limit for eserine of 0.368 μM (Rehák et al., 1997). The co-immobilization of AChE and ChO in a poly(amidoamine) dendrimers layer (Snejdarkova et al., 2003) decrease the detection limit for eserine to 0.03 ppb (0.1 nM).

The inhibition degree of AChE can be monitored through electrochemically oxidation of enzymatically generated thiocholine (TCh). On unmodified carbon-based electrodes, TCh is oxidized at high potential (+700 mV vs. Ag/AgCl) and the effect of any electrochemical interference species present in waste water samples cannot be removed. Various mediators, such as potassium ferrocyanide (Ivnitskii and Rishpon, 1994), cobalt phthalocyanine (Hart and Hartley, 1994), Prussian blue (Sun and Wang, 2010) and cobalt hexacyanoferrate (Arduini et al., 2009) have been reported in order to reduce the oxidation potential of TCh and increase the sensitivity of detection. Highly conductive nanomaterials such as carbon nanotubes were also reported to improve TCh detection (Liu and Lin, 2006; Merkoci et al., 2005).

* Corresponding author at: Department of Analytical Chemistry, University of Bucharest, 4-12 Regina Elisabeta Blvd., 030018 Bucharest, Romania. Tel./fax: +40 21 4104888.
E-mail address: camelia.bala@g.unibuc.ro (C. Bala).

0956-5663/$ - see front matter © 2013 Elsevier B.V. All rights reserved.
http://dx.doi.org/10.1016/j.bios.2013.02.018

The gels based on carbon nanotubes and imidazolium-based ionic liquids allowed the detection of TCh at a potential of +50 mV, with high sensitivity and detection limits between 50 and 80 μM TCh (Rotariu et al., 2010). The performances of these sensors were explained by the formation of composite materials with increased ionic conductivity based on electrostatic interaction between conjugated π electrons of the carbon material and the imidazolium cation (Fukushima and Aida, 2007).

Also, the tetrathiafulvalene–tetracyanoquinodimethane (TTF–TCNQ) charge-transfer complex can serve as an efficient electron donor and acceptor, due to the presence of four cyano groups and π conjugation. The TTF–TCNQ complex has been shown to be an effective mediator for several compounds such as hydrogen peroxide (Li et al., 1999), formaldehyde (Kataky et al., 2002) or glutathione (Calvo-Marzal et al., 2006). Novel gels with both electronic and ionic conductivities, obtained by mixing ionic liquids (IL) with TTF–TCNQ complex were reported (Mei and Ouyang, 2011) through a process similar to the preparation of gels of carbon nanotubes and ionic liquids (Fukushima, 2006). These gels are formed by a cation–π interaction between counterparts similar to carbon nanotube–ionic liquid gels and exhibit high conductivity. The TTF–TCNQ–ionic liquid composite gels present potential concern for electrochemistry and are very promising electrode material for biosensing.

This paper reports an AChE biosensor based on use of TTF–TCNQ–IL gel modified sensors for sensitive detection of carbamate drugs (Fig. S1). So far, this is the first biosensing application of this type of material. The TTF–TCNQ–IL gels have shown a significant signal enhancement effect for the anodic oxidation of thiocholine. Cyclic voltammetry, chronoamperometry and electrochemical impedance spectroscopy were used to characterize the TCh sensors. AChE was immobilized using sol–gel method on the gel modified sensor and the resulting biosensor was used for the detection of eserine and neostigmine. Easy and efficient biosensor regeneration was achieved using obidoxime.

2. Materials and methods

2.1. Reagents and materials

Acetylcholinesterase (from electric eel, 425.94 IU mg^{-1}) acetylthiocholine chloride (ATCh, purity ≥99%), 1-ethyl-3-methylimidazolium tetracyanoborate ([EMIM][TCB]), 1-ethyl-3-methylimidazolium trifluoromethanesulfonate ([EMIM][OTF]), 1-ethyl-3-methyl-imidazolium bis(trifluoromethylsulfonyl) amide ([EMIM][NTF_2]), 7,7,8,8-tetracyanoquinodimethane (TCNQ, purity 98%), tetrathiafulvalene (TTF, purity 97%), eserine (purity ≥99%), neostigmine bromide (purity ≥98%), obidoxime chloride (purity ≥95%), tetramethoxysilane (TMOS), methyltrimethoxysilane (MTMOS), polyethylene glycol (PEG600) were all purchased from Sigma-Aldrich. The carbon paste was supplied by Metrohm (66% graphite, 34% paraffin). All other reagents were of analytical grade. Acetylcholinesterase, acetylthiocholine and thiocholine solutions were prepared in phosphate buffer 0.1 M, pH 8. All solutions were prepared in ultrapure water (Millipore, 18 MΩ cm).

2.2. Instruments

Cyclic voltammetry, chronoamperometry measurements and electrochemical impedance spectroscopy (EIS) were all carried out using an AUTOLAB PGSTAT-12 potentiostat with a FRA2 module (Eco Chemie, Utrecht, The Netherlands) and the software used to gather data was GPES 4.9. The amperometric studies were carried out with a three-electrode cell which consists in a carbon paste electrode (diameter 3.0 mm) as working electrode, an Ag/AgCl 3 M KCl reference electrode and a Pt auxiliary electrode, all produced by Metrohm. Cyclic voltammetry experiments have been conducted at a scan rate of 100 mV s^{-1}, within the potential range of −400 to +800 mV. Amperometric measurements were performed at +400 mV vs. Ag/AgCl reference electrode. All experiments were carried out at room temperature (22 °C) using a 5 mL cell.

The FT-IR experiments were carried out on a Nicolet 4700 FT-IR spectrophotometer (Thermo Scientific). Scanning electron microscope (SEM) Carl Zeiss Auriga was used for the morphological analysis. Images were collected under 3.0 kV acceleration voltage and magnifications between 5000× and 50,000×.

2.3. Preparation of modified carbon paste sensors

Several types of carbon paste (CP) modified sensors were prepared: CP modified with TCNQ (TCNQ/CP), TTF (TTF/CP), TTF–TCNQ (TTF–TCNQ/CP), ILs (IL/CP) and TTF–TCNQ–IL gel (TTF–TCNQ–IL/CP). The CP electrode was first filled with carbon paste. An amount of carbon paste was removed from the top of the electrode to form a cavity of about 1 mm depth.

For the preparation of TCNQ/CP and TTF/CP sensors, 50 mg of TCNQ and TTF, respectively, were mixed with 200 μL acetonitrile and sonicated for 30 min (solutions A and B).

Equimolar amounts of TTF and TCNQ are reported for preparation of TTF–TCNQ complex related to the charge transfer inside the crystals (Mei and Ouyang, 2011). TTF and TCNQ have a weight ratio almost equal to their molar ratio and, consequently, the same quantity of the counterparts was used. The TTF–TCNQ mixture was prepared by grinding of 50 mg TTF and 50 mg TCNQ in an agate mortar for 5 min. Then 200 μL ACN was added and sonicated for 30 min (solution C). The TTF–TCNQ–IL gels were prepared by grinding TTF–TCNQ complex in different ionic liquids. 250 mg IL was added to 100 mg TTF–TCNQ into a mortar and the mixture was ground for 5 min (gel D). Preparation of the modified CP sensors was performed by casting of 5 μL solutions A, B, C and gel D respectively, on the CP electrodes cavity and left to dry for 30 min.

IL/CP electrodes were prepared according to a previous reported procedure (Rotariu et al., 2010).

2.4. Preparation of the biosensors

The immobilization of AChE on the modified TTF–TCNQ–IL/CP sensor was achieved using the sol–gel method using a procedure described earlier (Zamfir et al., 2011). The enzymatic activity was determined using the spectrophotometric Ellman method and 17 m IU were immobilized on the sensor surface. The biosensor was left to dry for 3–4 h at 4 °C and stored in phosphate buffer pH=8 at 4 °C.

2.5. Inhibition measurements

AChE activity was determined electrochemically by monitoring the formation of TCh in the hydrolysis reaction of ATCh both in the absence and after incubation with drug. The amperometric measurements were carried out in a PBS solution, pH 8, under stirring, at an applied potential of +400 mV. The addition of acethylthiocholine was made after the stabilization of the baseline current and the steady-state current was recorded. The biosensor was immersed either into the neostigmine or eserine solution for a period of time and then the oxidation current was measured by adding the same amount of substrate.

The inhibition degree was calculated using the formula

$$I\,(\%) = \left[(i_0 - i_I)/i_0\right] \times 100 \quad (1)$$

where i_0 and i_I are the currents for thiocholine oxidation measured before and after the contact of the biosensor with the drug.

The biosensor regeneration was performed by immersion in a 5 mM obidoxime solution under stirring. The biosensor was rinsed twice with ultrapure water and then with PBS to completely remove the obidoxime from the electrode surface. The regeneration degree was expressed using the formula

$$R\,(\%) = (i_R - i_I / i_0 - i_I) \times 100 \quad (2)$$

where i_R is the current recorded after reactivation with obidoxime, i_0 and i_I have the meaning that it was presented in Eq. (1).

3. Results and discussion

3.1. Cyclic voltammetry studies on TTF–TCNQ–IL modified CP sensors

Cyclic voltammetry was used to compare the electrochemical behavior of the composite mixtures with those of their counterparts. The six types of sensors presented in Section 2.4. were tested. EMIM salts were used in our experiments based on the fact that longer side alkyl chains, like butyl, do not form a gel with TTF–TCNQ complex (Mei and Ouyang, 2011).

The voltammograms recorded in TCh 5 mM for all types of electrodes are presented in Fig. 1. The oxidation potential of thiocholine decreases from +780 mV for [EMIM][OTF]/CP, +658 mV on the bare CP electrode to +615 mV for TTF/CP, +600 mV for TTF–TCNQ/CP, +415 mV for TCNQ/CP, +395 mV for TTF–TCNQ–[EMIM][TCB]/CP, +255 mV for TTF–TCNQ–[EMIM][NTF_2]/CP and +150 mV on TTF–TCNQ–[EMIM][OTF]/CP sensors.

Cyclic voltammogram of TTF–TCNQ/CP exhibit an oxidation peak at +600 mV and a reduction peak at around −259 mV. Oxidation process could be associated with the production of TTF^+ cation and free TCNQ. Oxidation is facilitated only if the TTF^+ is removed from the electrode surface for example by formation of a soluble or partial soluble salt TTF^+A^- (Zhao et al., 1992). According to some authors the use of PBS for electrochemical measurements seems to facilitate this process (Hill et al., 1990). On the other hand TCNQ could be reduced to a soluble salt based on the anion $TCNQ^-$. Removal of the radical anion is facilitated by the presence of alkaline cation with the formation of a salt MTCNQ. The cation TTF^+ and radical anion $TCNQ^-$ could also react to reform the initial complex TTF–TCNQ. Due to the ionic-conductivity the IL facilitates the migration of the cationic and anionic species inside the gel. Our electrochemical studies exhibited a lower oxidation and reduction potential for the TTF–TCNQ-[EMIM][TCB]/CP electrodes comparing with TTF–TCNQ/CP. The oxidation potential decrease from +600 mV for TTF–TCNQ/CP to +395 mV for TTF–TCNQ–[EMIM][TCB]/CP, while the reduction potential (data not shown) decrease from −259 mV for TTF–TCNQ/CP to −143 mV in the case of gel modified electrode. The enhanced electrocatalytic effect of the TTF–TCNQ–IL gels could be explained by the presence of the IL as a conductive matrix that allows the diffusion of the charged species originating from the electrochemical process inside the gel. The higher mobility for the TTF^+ inside the TTF–TCNQ–[EMIM][TCB] gel due to the presence of a small anion $[TCB]^-$ and the higher conductivity of the IL could also explain the enhanced electrocatalytical properties of this gel compared with the other two ILs used in our experiments.

The amount of IL in the gel was optimized in order to have a high and stable electrochemical signal for TCh detection. The ratio between the solid compounds and the IL was varied, while keeping constant the TTF:TCNQ ratio at 1:1. Composites with 1:1:2, 1:1:3, 1:1:5 (TTF:TCNQ:IL) ratios were tested. Ionic liquid loading affects the gel density. The gel became more solid-like at lower loading. For [EMIM][TCB] and [EMIM][OTF] modified sensors, the ratios of 1:1:2 and 1:1:3 were found to have low stability, the current substantially decreased after a number of 10 scans. For the [EMIM][OTF]-modified sensor with a ratio of 1:1:2 no peaks were observed, while for 1:1:3 ratio the oxidation potential for thiocholine is about +790 mV, much higher compared to value obtained for the 1:1:5 ratio of about +150 mV.

A gel based on low amount of IL seems to have a similar behavior as the IL/CP sensors. Increasing the ratio of IL in the gel leads probably to an enhancement of the ionic conductivity of the gel and consequently to an improvement of the electrocatalytic properties.

A high oxidation current was observed for the [EMIM][TCB]-modified sensor compared to other gel-modified sensors, which determined us to use this sensor for further development of the AChE biosensor. The sensor modified with TTF–TCNQ–[EMIM][TCB] gel prepared with a ratio of 1:1:5 was considered optimum and represents a compromise between a high peak current and a good stability of the signal.

3.2. Characterization of modified CP sensors

The formation of the TTF–TCNQ complex in free and after dispersion in an IL gel was checked by FT-IR spectroscopy. Literature provided several spectral evidences on the formation of such complex (Mei and Ouyang, 2011; Nanova et al., 2012). The results collected on pure TTF and TCNQ, and on free and [EMIM][TCB] dispersed TTF–TCNQ are presented in Fig. 2A.

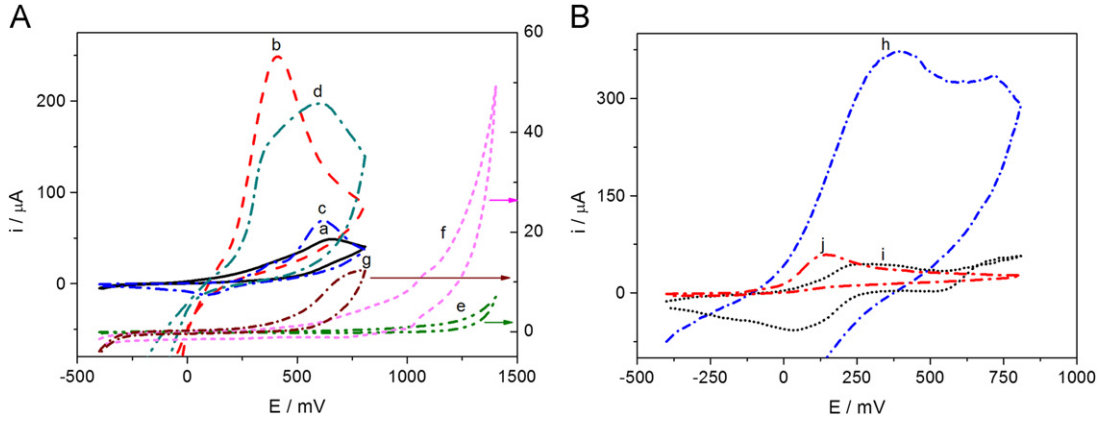

Fig. 1. Cyclic voltammograms for (A). Bare CP (a), TCNQ/CP (b), TTF/CP (c), TTF–TCNQ/CP (d), [EMIM][TCB]/CP (e)*, [EMIM][NTF_2]/CP (f)* and [EMIM][OTF]/CP (g)*. B. TTF–TCNQ–[EMIM][TCB]/CP (h), TTF–TCNQ–[EMIM][NTF_2]/CP (i) and TTF–TCNQ–[EMIM][OTF]/CP (j) (TCh 5 mM, SR=100 mV/s, pH=8). *Currents shown on the right axis.

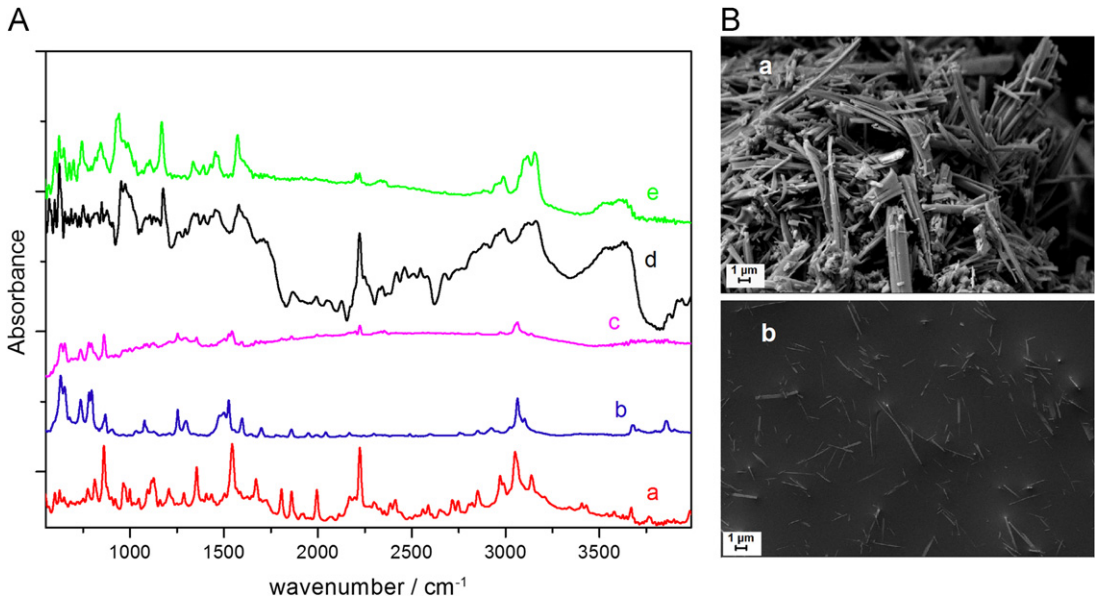

Fig. 2. A. FT-IR spectra of (a) TCNQ, (b) TTF, (c) TTF–TCNQ, (d) EMIMTCB, (e) TTF–TCNQ–EMIMTCB gel. B. SEM images of (a) TTF–TCNQ, (b) TTF–TCNQ–EMIMTCB gel.

The TCNQ spectrum presents a vibrational band at 2224 cm^{-1} attributed to the C≡N stretching. This band shifts to 2204 cm^{-1} in the TTF–TCNQ–[EMIM][TCB] and 2201 cm^{-1} in TTF–TCNQ spectra and confirms the presence of a negatively charged form of TCNQ in both mixtures. The presence of the TTF cation is proved by the shift of the vibrational band from 1525 cm^{-1} for neutral TTF, corresponding to C=C stretching, to 1542 cm^{-1} for the TTF–TCNQ–[EMIM][TCB] gel and TTF–TCNQ complex, while the band from 867 cm^{-1} disappears in both mixtures. The vibrational shifts of the bands observed in the spectrum of TCNQ and TTF in both physical mixtures (TTF–TCNQ and TTF–TCNQ–[EMIM][TCB] gel) may indeed account for the formation of such a complex.

The morphology of the TTF–TCNQ and TTF–TCNQ–[EMIM][TCB] gel was studied by SEM. One can observe from Fig. 2B, image a, the needle-like crystals microstructure of the TTF–TCNQ complex while image b shows the TTF–TCNQ–EMIMTCB gel with a well-defined dispersion of the crystals in the gel structure.

3.3. Amperometric measurements

Chronoamperometric measurements with the TTF–TCNQ–[EMIM][TCB] modified sensor were performed in phosphate buffer at different concentrations of thiocholine at a working potential of +400 mV vs. Ag/AgCl (Fig. 3A).

The catalytic rate constant k_{cat}, was calculated using the formula

$$i_{cat}/i_{buffer} = \pi^{1/2}(k_{cat}Ct)^{1/2} \quad (3)$$

where i_{cat} and i_{buffer} are the currents in the presence and absence of TCh, C is the TCh concentration and t is the time in second.

The catalytic rate constant was calculated from the slope of the plot i_{cat}/i_{buffer} vs. $t^{1/2}$ for a TCh concentration of 5 mM (inset Fig. 3A). A value of 32.3 L mol^{-1} s^{-1} was calculated for the gel based sensor, which reveals the fact that TTF–TCNQ–[EMIM][TCB] gel presents very good electrocatalytical properties towards thiocholine oxidation. This value is higher than the other reported in the literature for mediator modified electrodes (Arduini et al., 2009) but lower by comparison with electrodes modified with MWCNT–IL gel (Rotariu et al., 2010) or TCNQ–MWCNT based electrodes (Rotariu et al., 2012).

Chronoamperometric measurements allowed us also to estimate the thiocholine diffusion coefficient (D) based on Cottrel equation (Rotariu et al., 2010)

$$i = nFAD^{1/2}C/\pi^{1/2}t^{1/2} \quad (4)$$

The linear parts of the plots of i vs. $t^{-1/2}$ (Fig. 3B) were used to calculate the slope for each TCh concentration. The diffusion coefficient of $9.9 \cdot 10^{-7}$ cm^2 s^{-1} was determined from the plot ($It^{1/2}$) vs. C_{Tch}. A rapid diffusion of the analyte occurs at the electrode surface comparable with other TCh sensors based on IL gels and MWCNT (Rotariu et al., 2010) or TCNQ–MWCNT modified electrodes (Rotariu et al., 2012).

The calibration curve $i=f(C_{TCh})$ was obtained for the TTF–TCNQ–[EMIM][TCB] sensor by successive additions of TCh in a concentration range between 0.05 and 6 mM TCh. A linear response was recorded in the range 0.05–2.5 mM TCh with a sensitivity of 55.9 ± 1.2 μA mM^{-1} cm^{-2} and a detection limit of 7.6 μM. Sensitivity is higher and detection limit is lower comparing with TCh sensors previously reported (Rotariu et al., 2010, 2012).

3.4. Electrochemical impedance spectroscopy study

The electrochemical properties of the TTF–TCNQ–EMIMTCB gel were also investigated using electrochemical impedance spectroscopy. Two types of redox couples were used, one negatively charged $[Fe(CN)_6]^{3-}/[Fe(CN)_6]^{4-}$ and one positively charged, $[Ru(NH_3)_6]^{2+}/[Ru(NH_3)_6]^{3+}$. The measurement of the electron-transfer resistance gave us information about the electron transfer kinetic at the electrode/electrolyte solution interface.

Fig. 4A shows the Nyquist plots of the couple $[Fe(CN)_6]^{3-}/[Fe(CN)_6]^{4-}$ for unmodified CP and TCNQ, TTF, TCNQ–TTF, [EMIM][TCB] and TTF–TCNQ–[EMIM][TCB] modified sensors. The plots show a semicircular domain at high frequencies and a linear one at low frequencies. The first domain corresponds to an electron transfer process at the electrode surface and the second one to a diffusion process. A Randles circuit was used to fit the impedance data plots. The impedance values were found to be quite similar for the CP and the TTF/CP electrodes, $3.94 \pm 0.21 \times 10^3$ Ω for unmodified electrode and $4.21 \pm 0.22 \times 10^3$ Ω for TTF/CP, respectively. TCNQ modified electrode exhibited a lower resistance to electron transfer for negatively charged redox couple of 547 ± 15 Ω. The

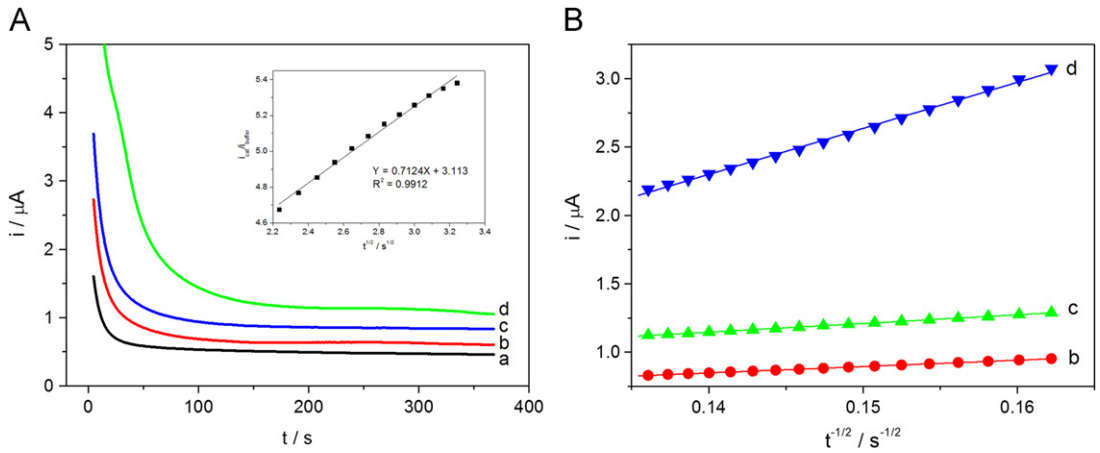

Fig. 3. A. Chronoamperograms using TTF–TCNQ–EMIMTCB/CP electrode in the absence (a), and presence of TCh 1 mM (b), 2 mM (c), 5 mM (d) (PBS, pH=8). Inset: plot i_{cat}/i_{buffer} vs. $t^{1/2}$ derived from chronoamperometric data for TCh 5 mM (d) and buffer (a). B. Linear segments of the plot i vs. $t^{-1/2}$ for TCh 1 mM (b), 2 mM (c) and 5 mM (d).

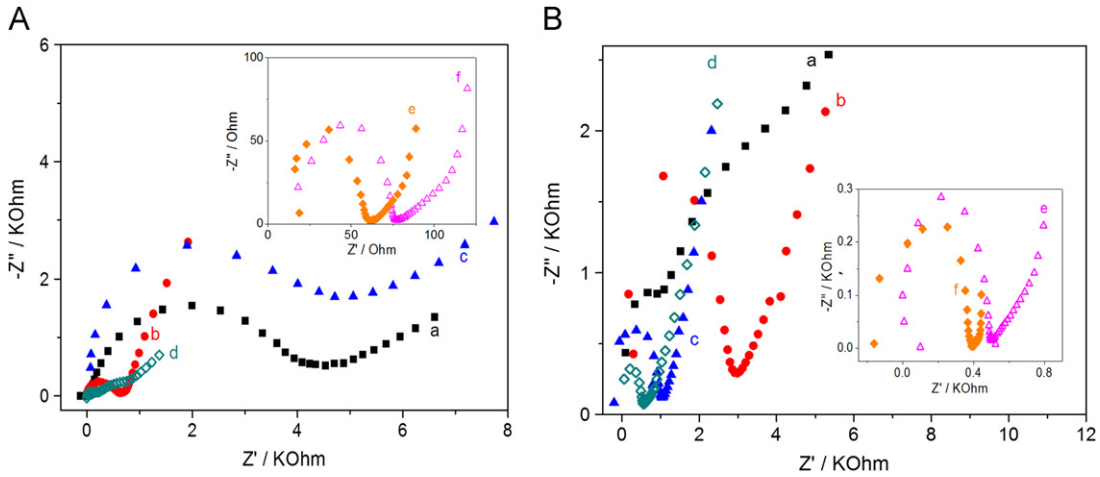

Fig. 4. A. Nyquist plots for the CP (a), TCNQ/CP (b), TTF/CP (c) and CP–EMIMTCB/CP (d) in the presence of 2.5 mM $Fe(CN)_6^{3-}/Fe(CN)_6^{4-}$ Inset: Nyquist plots TTF–TCNQ/CP (e) and TTF–TCNQ–EMIMTCB/CP (f). B. Nyquist plots for the CP (a), TCNQ/CP (b), TTF/CP (c) and CP–EMIMTCB/CP (d) in the presence of 2.5 mM $Ru(NH_3)_6^{2+}/Ru(NH_3)_6^{3+}$ Inset: Nyquist plots TTF–TCNQ/CP (e) and TTF–TCNQ–EMIMTCB/CP (f) (frequency range from 0.01 kHz to 1 MHz, perturbation signal of 5 mV, OCP).

presence of the organic conducting salt TTF–TCNQ leads to a decrease of the resistance to $244 \pm 12\ \Omega$. The lowest impedance of $20.9 \pm 1.3\ \Omega$ was observed for TTF–TCNQ–[EMIM][TCB]/CP sensor. The formation of the composite gel, positively charged due to the imidazolium cation, can explain this behavior. Electrostatic interaction between the positively charged electrode surface and the negatively charged redox couple $[Fe(CN)_6]^{3-}/[Fe(CN)_6]^{4-}$ favors the electron transfer.

These results demonstrate that interaction of the negatively charged species with the electrode surface is favored in the presence of TTF–TCNQ–EMIM][TCB] gel. The significant decrease in impedance indicates the existence of synergistic effect between the mediators and ionic liquid, compared to the TTF–TCNQ complex. A similar electrochemical process is expected for TCh oxidation at pH 7.4 at the surface of the electrode.

A similar experiment was carried out using the $[Ru(NH_3)_6]^{2+}/[Ru(NH_3)_6]^{3+}$ redox couple. In the case of a positively charge couple TTF/CP presented a lower resistance ($970 \pm 35\ \Omega$) compared to TCNQ/CP ($2.28 \pm 0.12 \times 10^3\ \Omega$). This is quite the opposite behavior if we look to the EIS results for ferri/ferrocyanide. An improvement of the electron transfer was obtained by using the TTF–TCNQ modified electrode. The resistance decreased to $467 \pm 16\ \Omega$. The lowest impedance was observed for gel modified sensor with a resistance of $295 \pm 10\ \Omega$. Compared to the resistance value measured for the ferri/ferrocyanide redox couple the impedance measured for the $[Ru(NH_3)_6]^{2+}/[Ru(NH_3)_6]^{3+}$ couple is approximately ten times higher, proving that the composite gel is much more favorable for an electron transfer between a negatively charged species and the electrode surface than between a positively one and electrode. One can say that ionic conductivity of the electrode material, due to the presence of ionic liquid, is decisive for the electrochemical properties of the TTF–TCNQ–[EMIM][TCB] gel. This can also explain the cyclic voltammetry results, respectively the enhancement of the electrocatalytical properties toward TCh oxidation by increasing the ratio of ionic liquid in the gel.

3.5. Biosensor calibration for ATCh

Amperometric measurements were carried out at a working potential of +400 mV by successive additions of ATCh in PBS using the AChE biosensors. The biosensor calibration was performed in the concentration range of 0.1–5 mM ATCh. A fast response of 10 s was observed, which shows the absence of any diffusional limitation toward the enzymatic the hydrolysis reaction. A typical Michaelis–Menten process was observed with a linear increase of the amperometric signal until 4 mM ATCh and a flattening trend for higher concentrations.

Neostigmine and eserine detection was performed by measuring the enzyme activity in the absence and after incubation with

the drug. A saturation of the enzyme catalytic sites, necessary for determination of the enzyme activity, was achieved by selection of the working substrate concentration in the plateau region of the calibration curve. A concentration of 5 mM ATCh was considered to assure saturation of the enzyme with substrate. The biosensors were stored at 4 °C in PBS solution in order to preserve the enzyme activity immobilized in sol–gel matrix (Zamfir et al., 2011).

Reproducibility of analytical signal recorded in the presence of 5 mM ATCh was tested with five different biosensors from the same batch. The RSD value equal to 5.9% reveals a good reproducibility of the biosensor. Intra-assay reproducibility is expressed by a relative standard deviation of 3.6% for five determinations on ATCh 5 M by using the same biosensor. Storage stability was determined by performing five successive determinations on ATCh 5 mM every day on the same biosensor. The biosensor was kept at 4 °C between the measurements and from 1 day to another. The signal reaches 92% from the initial value after 2 weeks, indicating a good stability of the AChE biosensor.

3.6. Neostigmine and eserine detection with the TTF–TCNQ–EMIMTCB/CP biosensors

Two important carbamate therapeutic drugs, eserine and neostigmine were used as inhibitors for biosensing tests. Inhibition measurements were performed on 10^{-6} M eserine in order to optimize the incubation time (5–30 min). The inhibition degree increases with the incubation time from 5% to 100% for eserine. These results is in agreement with the other previously reported data (Kordaš et al., 1975). The calibration curves for eserine and neostigmine were obtained using a 30 min incubation period. The calibration curves were linearized using the semi-logarithmic representation $I\% = f(\log C)$. The main calibration parameters are presented in Table 1.

The detection limits calculated were 26 pM (7 ppt) eserine and 0.3 nM (57 ppt) neostigmine for an inhibition degree of 10%. From our knowledge these values represent the lowest detection limits reported in the literature for these compounds. For instance, AChE interaction with SPR detection allowed a detection of neostigmine down to a concentration of 10 μM, while eserine was detectible only at 50 μM (Milkani et al., 2011). Acetylcholinesterase–ISFET based system was able to detect eserine from 0.1 μM (Hai et al., 2006). Detection of eserine by HPLC with UV detection was performed starting with 2 ng/nL (2 ppb) (Varin et al., 1999). Ghous et al. reported a LOD for serine of 70 ppb using a method based on capillary electrophoresis (Havel et al., 2002). Detection limits of 30 ppt have been reported by using an AChE biosensor based on dendrimer layers (Snejdarkova et al., 2003). Detection of these compounds at lower concentrations is justified by the applications in waste water analysis and clinical analysis.

Rinsing with buffer did not allow us to have a fast and complete regeneration of the biosensors as some other authors reported (Wilson et al., 1961). Regeneration experiments were performed with obidoxime 5 mM for a time period ranging from 5 to 30 min. The use of obidoxime was justified by the need to completely break the covalent bonds of the enzyme–inhibitor complex. An incubation time of 30 min with obidoxime 5 mM was found to be optimum for a complete regeneration on the entire concentrations range of tested drugs. After each inhibition measurement, the biosensor was immersed into 5 mM obidoxime solution for 30 min under stirring and then washed twice with ultrapure water and once with buffer solution.

The reproducibility of the inhibition was tested on eserine 10^{-8} M. For five successive inhibition–regeneration cycles on the same biosensors, a reproducibility of 6% was achieved, showing a good reproducibility of the inhibition determination. Lower detectable concentration of carbamates drugs achieved by the AChE biosensor reported in this work allows the analysis of these compounds in wastewaters. Real sample analysis was realized by spiking the tap water samples with known amounts of drugs. Tap water sample analysis led to an inhibition degree below the detection limit. Further, the inhibition tests were performed by adding different amounts of eserine and neostogmine in tap water samples. Spiked water samples with drug concentrations of 10, 50 and 100 nM were analyzed and the experimental results are presented in Table 2.

The inhibition degrees were in good correlation with those produced by standard solutions and indicated a good accuracy of the biosensor. The percentage of the recovery calculated as the ratio between inhibition degree of spiked sample and respectively standard solution was between 85% and 114% for both drugs. A lower recovery of about 78% and low precision (21%) was obtained only for neostigmine 10 nM. These results confirm that the biosensor presented in this work could be used for screening of water samples in detection of carbamate drugs.

4. Conclusions

The use of TTF–TCNQ–IL gels for development of thiocholine sensors is presented in this work. SEM and FT-IR studies have revealed the morphological modifications during the preparation steps and the interactions between the counterparts. Depending on the ionic liquid used, the TCh oxidation potentials were found to be between +150 and +400 mV vs. Ag/AgCl. CV and EIS experiments demonstrated that ionic conductivity plays an important role and explain the electrochemical properties of the gel modified electrodes. Electrochemical studies proved that TTF–TCNQ–[EMIM][TCB] presented the highest sensitivity for TCh detection and was further used for development of AChE biosensor for carbamate drugs detection. Chronoamperometric determinations allowed to estimate the catalytic constant and diffusion coefficient for TCh, which are ones of the highest reported in the literature. The enzyme AChE was immobilized on the surface of the TTF–TCNQ–[EMIM][TCB]/CP electrode using sol–gel technique. Detection of eserine and neostigimine was realized for an

Table 1
Eserine and neostigmine detection with AChE biosensors based on TTF–TCNQ–EMIMTCB/CP; $I\% = a + b \times \log C_{compound}$ (M) (incubation time = 30 min).

Pesticide	a	b	R	Conc. range (nM)	LOD[a]	
					nM	ppt
Eserine	220.4 ± 13.6	19.9 ± 1.7	0.9645	0.1–1000	2.6×10^{-2}	7
Neostigmine	247.2 ± 21.9	24.8 ± 2.8	0.9504	1–500	0.3	57

[a] $I = 10\%$

Table 2
Eserine and neostigmine spiked tap water samples analysis.

Drug	Drug added (nM)	Inhibition degree (%)		Recovery (%)
		Standard solution	Spiked tap water	
Eserine	10	61	54 ± 4	85.8 ± 7.4
	50	75	70 ± 4	96.2 ± 5.7
	100	81	93 ± 4	114.4 ± 4.3
Neostigmine	10	49	38 ± 8	78 ± 21
	50	66	65 ± 1	97.8 ± 1.5
	100	74	76 ± 4	103.2 ± 5.2

$n = 3$

extended range starting with 0.1 nM and 1 nM, respectively. Very low detection limits of 26 pM eserine and 0.3 nM neostigimine were achieved. The proposed biosensor exhibited a high sensitivity and efficient reactivation of the enzyme. The analysis of spiked tap water has revealed a good recovery degree for both drugs that have been tested and proved the capability to be used as a screening method for detection of carbamates drug in wastewaters.

Acknowledgments

This work was supported by a grant of the Romanian National Authority for Scientific Research, projects PN-II-ID-PCE-2011-3-0286. L.-G. Zamfir is grateful to the grant POSDRU 107/1.5/S/80765 for the doctoral fellowship. We thank Dr. Virgil Marinescu from ICPE-CA for SEM images recording.

Appendix A. Supporting information

Supplementary data associated with this article can be found in the online version at http://dx.doi.org/10.1016/j.bios.2013.02.018.

References

Amine, A., Mohammadi, H., Bourais, I., Palleschi, G., 2006. Biosensors and Bioelectronics 21 (8), 1405–1423.
Andreescu, S., Marty, J.-L., 2006. Biomolecular Engineering 23 (1), 1–15.
Arduini, F., Cassisi, A., Amine, A., Ricci, F., Moscone, D., Palleschi, G., 2009. Journal of Electroanalytical Chemistry 626 (1–2), 66–74.
Calvo-Marzal, P., Chumbimuni-Torres, K.Y., Höehr, N.F., Kubota, L.T., 2006. Clinica Chimica Acta 371 (1–2), 152–158.
Darvesh, S., Hopkins, D.A., Geula, C., 2003. Nature Reviews Neuroscience 4 (2), 131–138.
Fukushima, T., 2006. Polymer Journal 38 (8), 743–756.
Fukushima, T., Aida, T., 2007. Chemistry—A European Journal 13 (18), 5048–5058.
Ghous, T., Townshend, A., 1998. Analytica Chimica Acta 372 (3), 379–386.
Hai, A., Ben-Haim, D., Korbakov, N., Cohen, A., Shappir, J., Oren, R., Spira, M.E., Yitzchaik, S., 2006. Biosensors and Bioelectronics 22 (5), 605–612.
Hart, J.P., Hartley, I.C., 1994. Analyst 119, 259–263.
Havel, J., Patočka, J., Bocaz, G., 2002. Journal of Capillary Electrophoresis and Microchip Technology 7 (5–6), 107–112.
Hill, B.S., Scolari, C.A., Wilson, G.S., Bartlett, P.N., Albery, W.J., 1990. Philosophical Transactions of the Royal Society of London 333 (1628), 63–69.
Ivnitskii, D.M., Rishpon, J., 1994. Biosensors and Bioelectronics 9 (8), 569–576.
Kataky, R., Bryce, M.R., Goldenberg, L., Hayes, S., Nowak, A., 2002. Talanta 56 (3), 451–458.
Kordaš, M., Brzin, M., Majcen, Ž., 1975. Neuropharmacology 14 (11), 791–800.
LeDoux, M., 2011. Journal of Chromatography A 1218 (8), 1021–1036.
Li, Q.-S., Ye, B.-C., Liu, B.-X., Zhong, J.-J., 1999. Biosensors and Bioelectronics 14 (3), 327–334.
Liu, G., Lin, Y., 2006. Analytical Chemistry 78 (3), 835–843.
Mei, X., Ouyang, J., 2011. Langmuir 27 (17), 10953–10961.
Merkoci, A., Pumera, M., Llopis, X., Perez, B., del Valle, M., Alegret, S., 2005. TrAC Trends in Analytical Chemistry 24 (9), 826–838.
Milkani, E., Lambert, C.R., McGimpsey, W.G., 2011. Analytical Chemistry 408 (2), 212–219.
Nanova, D., Beck, S., Fuchs, A., Glaser, T., Lennartz, C., Kowalsky, W., Pucci, A., Kroeger, M., 2012. Organic Electronics 13 (7), 1237–1244.
Rehák, M., Šnejdárková, M., Hianik, T., 1997. Electroanalysis 9 (14), 1072–1077.
Rotariu, L., Zamfir, L.-G., Bala, C., 2010. Sensors and Actuators B 150 (1), 73–79.
Rotariu, L., Zamfir, L.-G., Bala, C., 2012. Analytica Chimica Acta 748, 81–88.
Rubnov, S., Levy, D., Schneider, H., 1999. Journal of Pharmaceutical and Biomedical Analysis 18 (6), 939–945.
Snejdarkova, M., Svobodova, L., Nikolelis, D.P., Wang, J., Hianik, T., 2003. Electroanalysis 15 (14), 1185–1191.
Sun, X., Wang, X., 2010. Biosensors and Bioelectronics 25 (12), 2611–2614.
Varin, F., Couture, J., Gao, H., 1999. Journal of Chromatography B 723 (1–2), 319–323.
Wilson, I.B., Harisson, M.A., Ginsburg, S., 1961. Journal of Biological Chemistry 236 (5), 1498–1500.
Zamfir, L.-G., Rotariu, L., Bala, C., 2011. Biosensors and Bioelectronics 26 (8), 3692–3695.
Zhao, S., Korell, U., Cuccia, L., Lennox, R.B., 1992. Journal of Physics and Chemistry 96 (13), 5641–5652.